Cannabinoid modulation of limbic forebrain noradrenergic circuitry

Ana Franky Carvalho[1,2], **Kenneth Mackie**[3], and **Elisabeth J. Van Bockstaele**[1]

[1]Neurosurgery, Farber Institute for Neurosciences Thomas Jefferson University Philadelphia, PA, USA

[2]Life and Health Science Research Institute (ICVS) School of Health Sciences, University of Minho Braga, Portugal

[3]Psychological and Brain Sciences Indiana University Bloomington, IN, USA

Abstract

Both the endocannabinoid and noradrenergic systems have been implicated in neuropsychiatric disorders. Importantly, low levels of norepinephrine are seen in patients with depression and antagonism of the cannabinoid receptor type 1 (CB1R) is able to induce depressive symptoms in rodents and humans. Whether the interaction between the two systems is important for the regulation of these behaviors is not known. In the present study, adult male Sprague-Dawley rats were acutely or chronically administered the CB1R synthetic agonist, WIN 55,212-2, and α2A and β1 adrenergic receptors (AR) were quantified by western blot. These AR have been shown to be altered in a number of psychiatric disorders and following antidepressant treatment. CB1R agonist treatment induced a differential decrease of α2A- and β1-ARs in the nucleus accumbens (Acb). Moreover, to assess long lasting changes induced by CB1R activation, some of the chronically treated rats were euthanized seven days following the last injection. This revealed a persistent effect on α2A-AR levels. Furthermore, the localization of CB1R with respect to noradrenergic profiles was assessed in the Acb and in the nucleus of the solitary tract (NTS). Our results show a significant topographic distribution of CB1R and dopamine beta hydroxylase immunoreactivities in the Acb with higher co-localization observed in the NTS. In the Acb, CB1R-ir was found in terminals forming either symmetric or asymmetric synapses. These results suggest that cannabinoids may modulate noradrenergic signaling in the Acb by acting on noradrenergic neurons in the NTS or indirectly by modulating inhibitory and excitatory input in the Acb.

Keywords

Cannabinoid receptor type1; adrenergic receptor; nucleus accumbens; nucleus of the solitary tract; Sprague-Dawley

INTRODUCTION

The cannabinoid receptor type 1 (CB1R) can be found in several areas of the brain such as the frontal cortex, basal ganglia, hippocampus, amygdala and brainstem (Mackie, 2005) and it has been implicated in the regulation of learning and memory as well as depression, anxiety and pain. CB1R activation is known to inhibit GABA and glutamate release in several brain regions, including the hippocampus, dorsal striatum, cerebellum and nucleus

Corresponding author: Ana Franky Carvalho Neurosurgery Farber Institute for Neurosciences Thomas Jefferson University 900 Walnut Street, Suite 417 Philadelphia, PA 19107 Phone: (215) 503-9147 arfranky@gmail.com.

accumbens (Acb) (Hoffman & Lupica, 2000; Daniel & Crepel, 2001; Gerdeman & Lovinger, 2001; Robbe *et al.*, 2001). In addition to the effects of cannabinoids on GABA and glutamate transmission, growing evidence points to a significant role for monoamines in cannabinoid-induced behaviors. Previous studies have shown important interactions between the cannabinoid and noradrenergic systems (Oropeza *et al.*, 2005, 2007; Page *et al.*, 2007; Fox *et al.*, 2009; Jelsing *et al.*, 2009). Systemic administration of the synthetic cannabinoid agonist, WIN 55,212-2, was shown to increase the release of norepinephrine (NE) in the prefrontal cortex (PFC) (Oropeza *et al.*, 2005). In addition, WIN 55,212-2 increased c-fos expression in the locus coeruleus (LC) and in the nucleus of the solitary tract (NTS) (Oropeza *et al.*, 2005; Jelsing *et al.*, 2009). Efferents of the LC and the NTS account for most of the noradrenergic projections to the forebrain. The noradrenergic input to cortical and limbic structures is important for brain arousal, memory and mood (Aston-Jones *et al.*, 1991; Heninger *et al.*, 1996). Dysregulation of this system plays a role in the pathophysiology of depression (Heninger *et al.*, 1996; Anand & Charney, 2000; Nutt, 2002). Noradrenergic deficiency and dysfunction of adrenergic receptors (AR) may be present in some patients with depression and may be important for the response to antidepressants (Anand & Charney, 2000). Consistent with this, various studies show an increase in α2-AR density in brains of depressed suicide victims (Meana *et al.*, 1992; De Paermentier *et al.*, 1997; Callado *et al.*, 1998) while β1-AR density is decreased (De Paermentier *et al.*, 1990). With regard to antidepressant treatment, the levels of α2- and β1-ARs have been shown to decrease (De Paermentier *et al.*, 1991., 1997) in areas such as temporal cortex, amygdala and thalamus of antidepressant-treated suicides. Moreover, chronic administration of WIN 55,212-2 has been shown to desensitize α2-ARs in noradrenergic enriched areas (Moranta *et al.*, 2009). Elucidating the effects of cannabinoid administration on the expression of these ARs may contribute to identifying the mechanism by which cannabinoids are involved in mood-related disorders (Hill & Gorzalka, 2005a; Witkin *et al.*, 2005; Leweke & Koethe, 2008).

In the present study, we studied the impact of a cannabinoid agonist on limbic forebrain noradrenergic circuitry using biochemical and neuroanatomical approaches. The limbic region analyzed, the Acb, is a brain region involved in the integration of motivation-related information, with important implications for drug addiction and mood disorders (Di Chiara, 2002; Shirayama & Chaki, 2006). Understanding how cannabinoids may impact noradrenergic input to the Acb may provide important information regarding the effects of CB1R compounds on drug-induced behaviors.

MATERIALS AND METHODS

Subjects

Adult male Sprague-Dawley rats (Harlan Laboratories, Indianapolis, IN) weighting 220–250g were housed two or three per cage in a controlled environment (12-hour light schedule, temperature at 20°C). Food and water were provided *ad libitum*. The care and use of animals were approved by the Institutional Animal Care and Use Committee (IACUC) of Thomas Jefferson University and were conducted in accordance with the NIH *Guide for the care and use of laboratory animals*. All efforts were made to minimize animal suffering and reduce the number of animals used.

Antibody characterization and specificity

A list with the characterization of all the primary antibodies used can be found in table 1.

An affinity-purified polyclonal antibody directed against the CB1R was used that was generated against a fusion protein containing the last 15 amino acids of the C-terminal of the

rat CB1R fused to glutathione *S*-transferase. The specificity of this CB1R antibody has been determined in somatosensory cortex of mice lacking CB1R by (Bodor *et al.*, 2005). In addition to the aforementioned study, additional controls were conducted here. For example, immunoperoxidase detection of the CB1R antibody was conducted in tissue sections obtained from the forebrain of mice deficient in the CB1R (provided by Kenneth Mackie) and compared to that of comparable sections obtained from wild type mice. In these experiments, peroxidase detection for CB1R was absent in knockout tissue but present in wild type samples (Fig. 1). In addition, specificity controls involved controlling for the secondary antibody by processing tissue that lacked primary antibody incubation. In such experiments, ran in parallel, peroxidase immunoreactivity or immunogold-silver particles were not detected in tissue sections where the primary antibody was omitted (S1). To evaluate possible cross-reactivity of secondary antibodies with the primary antisera in the dual labeling experiments, some sections were processed for dual labeling with omission of one of the primary antisera.

The monoclonal antibody against the dopamine beta hydroxylase (DBH) was raised against purified bovine DBH. The specificity of the DBH antibody has also been demonstrated previously in our laboratory (Oropeza *et al.*, 2007). More specifically, preabsorption with the respective antigen (Alpha Diagnostics, San Antonio, TX) resulted in an absence of immunolabeling in tissue sections from the frontal cortex.

The monoclonal (clone CL-300) antibody directed against calbindin was generated using the purified Calbindin-D from chicken gut. This antibody revealed the same distribution in the Acb as described by others (Voorn *et al.*, 1989; Jongen-Relo *et al.*, 1994).

The monoclonal antibody direct against the NE transporter (NET) was generated using a peptide (amino acids 05–17) of the mouse and rat NET coupled to keyhole limpet hemocyanin (KLH) by the addition of a C-terminal cysteine. To test the specificity of the NET antibody, preabsorption of the antibody with the blocking peptide (1μg/ml, MabTechnologies, Stone Mountain, GA) resulted in the absence of immunolabeling in rat tissues containing the Acb (S2).

The polyclonal antibody against the α2A-AR was developed against a synthetic peptide (Arg-Ile-Tyr-Gln-Ile-Ala-Lys-Arg-Arg-Thr-Arg-Val-Pro-Pro-Ser-Arg-Arg-Gly) derived from amino acids 218–235 of human, mouse, rat and pig α2A-AR. The polyclonal antibody against the β1-AR was raised against a synthetic peptide (His-Gly-Asp-Arg-Pro-Arg-Ala-Ser-Gly-Cys-Leu-Ala-Arg-Ala-Gly) derived from amino acids 394–408 of mouse and rat β1-AR. The specificity of α2A- and β1-AR antibodies was determined by preabsorption of the antibodies with the respective blocking peptide (10μg/ml, Sigma-Aldrich, St. Louis, MO) that resulted in absence of labeling in the blots loaded with whole brain protein samples (S3).

The monoclonal antibody against microtubule associated protein (MAP2) was raised in mouse against rat brain MAP. The specificity of the MAP2 antibody has been described (Teng *et al.*, 2001) where there was no detectable band in western blot from brain extracts of MAP2 deficient mice.

Drug administration and Western blot analysis

WIN 55,212-2 (Sigma-Aldrich) was dissolved in 5% dimethyl sulfoxide (DMSO)(Fisher Scientific, Fair Lawn, NJ) in 0.9% saline and injected intraperitoneally in a volume of 1ml/kg body weight. A dose-response study was performed in which animals received an acute injection of WIN 55,212-2 at 0.3, 1.0, 3.0 or 7.0 mg/kg (n=20) or vehicle (5% DMSO in saline, n=5). Another set of animals was divided in 3 treatment groups (acute, chronic and

chronic+abstinence). In the acute group, animals received one injection of 3.0 mg/kg WIN 55,212-2 (n=8) or vehicle (n=6). The chronic group received a daily injection of WIN 55,212-2 (n=8) or vehicle (n=6) for 7 days. Animals in the dose-response study and in the acute and chronic groups were euthanized 40 to 45 minutes after the last injection. The chronic+abstinence group received repeated injections (7 days) of WIN 55,212-2 (n=8) or vehicle (n=6) and were euthanized 7 days after the last injection. Experimental animals were anesthetized with isoflurane (Isoflurane, USP, Webster Veterinary, Sterling, MA) and decapitated. Brains were removed and a coronal section containing the whole extension of the Acb (approximately from +0.7mm to +2.7mm anterior to bregma) was cut. The area punched was located medially to the anterior commissure and ventrally to the lateral ventricle, including the shell and medial core of the Acb (as shown in Fig. 2). Part of the cerebellum was also collected from a coronal section approximately from −10.50mm to −12mm posterior to bregma. Proteins were extracted in radio immunoprecipitation assay (RIPA) lysis buffer (Santa Cruz Biotechnology, Santa Cruz, CA). Protein quantification was performed using the bicinchoninic acid (BCA) reagent. Protein samples were loaded at equal concentrations and ran on a 4–12% Tris-glycine gel (Invitrogen, Carlsbad, CA). Gels were then transferred to Immobilon-P polyvinylidene difluoride (PVDF) membranes (Millipore Corp., Bedford, MA) at 25V for 2 hours. Membranes were probed for rabbit anti-α2A-AR (1:500, Sigma-Aldrich), rabbit anti-β1-AR (1:1000, Sigma-Aldrich) or mouse anti-NET (1:5000, MabTechnologies) using the Western Breeze Chemilluminescent Kit (Invitrogen). In order to control for protein loading, each blot was stripped using Restore Stripping Buffer (Pierce, Rockford, IL) and re-probed for β-actin (1:5000, Sigma-Aldrich).

Light microscopy and immunofluorescence

Seven naïve animals were used for light and immunofluorescence microscopy. Animals were deeply anesthetized with sodium pentobarbital (60 mg/kg) administered intraperitoneally and transcardially perfused with 50ml of heparinized saline followed by 400ml of 4% formaldehyde (Electron Microscopy Sciences, Fort Washington, PA) in 0.1M phosphate buffer (PB, pH7.4). After perfusion, brains were removed and postfixed in the same fixative. Coronal sections throughout the Acb and the NTS were cut at 40μm using a Vibratome (Technical Product International, St Louis, MO, USA) and collected into 0.1M PB. Every sixth section of the Acb was processed for immunohistochemical visualization of calbindin, CB1R or DBH immunoreactivities. Free-floating sections were treated with 1% sodium borohydride in 0.1M PB for 30 min. They were then rinsed with 0.1M PB and later washed in 0.1M Tris saline buffer (TS, pH 7.6). The sections were blocked in 0.5% bovine serum albumin (BSA) in 0.1M TS for 30 min and then washed for 5 min, twice. Sections were incubated overnight at room temperature with a mouse antibody for calbindin (1:300, Abcam, Cambridge, MA), a rabbit antibody directed against CB1R (1:500) or a mouse monoclonal antibody recognizing DBH (1:1000, Chemicon, Millipore) in 0.1% BSA/0.25% Triton-X 100 in 0.1M TS. The sections were then washed in 0.1M TS, three times for 10 min. Then, sections were incubated in a secondary biotin-conjugated donkey anti-rabbit or donkey anti-mouse IgG (1:400, Jackson ImmunoResearch, West Grove, PA) in 0.1% BSA/ 0.25% Triton-X 100 in 0.1M TS for 30 min at room temperature. Then sections were washed in 0.1M TS, three times for 10 min. Sections were incubated in an avidin-biotin complex solution (VECTASTAIN Elite ABC Kit, Vector Laboratories, Burlingame, CA) in 0.1M TS for 30 min and then washed. CB1R and DBH immunoreactivity was visualized by a red reaction by incubating the tissue sections in a red peroxidase substrate (VECTOR NovaRED substrate kit, Vector Laboratories, Burlingame, CA) for 5 min, while the calbindin immunoreactivity was visualized by a blue reaction by incubating the sections in a blue peroxidase substrate (VECTOR SG substrate kit) for 10 min. The reaction was stopped by rinsing the sections in distilled water and then the sections were washed in 0.1M TS. For dual immunofluorescence, every sixth section of Acb and NTS was processed as described

above except that tissues were incubated overnight in a cocktail with rabbit anti-CB1R (1:500 for Acb sections, 1:5000 for NTS sections) and mouse anti-DBH antibodies or rabbit anti-CB1R and mouse anti-MAP2 (1:1000, Abcam) in 0.1% BSA+2% TritonX- 100 in 01.M TS. Then, tissues sections were incubated in a secondary antibody solution containing fluorescein isothiocyanate (FITC) donkey anti-mouse IgG (1:200, Jackson ImmunoResearch) and tetramethyl rhodamine isothiocyanate (TRITC) anti-rabbit IgG (1:400, Jacskon ImmunoResearch) in 0.1% BSA+2% Triton-X 100 in 0.1M TS, for 2 hours at room temperature. Sections were then washed in 0.1M PB. Both dual and single labeled sections were mounted onto gelatinized glass slides from a 0.05M PB solution. The slides were dehydrated through a graded series of alcohols and cleared in xylene before being coverslipped with Permount (light microscopy) (Fisher Scientific, Pittsburgh, PA) or DPX (immunofluorescence) (Sigma-Aldrich) mounting mediums.

Electron microscopy

Although DBH was an adequate marker for noradrenergic terminals using light and fluorescence microscopy because of the ability to increase penetration with detergents in thicker tissue section, this vesicular-bound enzyme was more difficult to consistently detect using electron microscopy with low concentrations of permeabilization agents. Therefore, without using detergents, NET was used as a marker to detect noradrenergic axon terminals and did not compromise the ultrastructural preservation of the neuropil. NET and CB1R were visualized in sections through the Acb obtained from naïve rats (n=7) that were perfused with 50ml of heparinized saline followed by 100ml 3.8% acrolein (Electron Microscopy Sciences) and 400ml of 2% formaldehyde (Electron Microscopy Sciences) in 0.1M PB. Sections were processed following the protocol described for light microscopy except that Triton-X 100 was not added to the solution for antibody incubation. The sections were incubated overnight, at room temperature, in a primary antibody solution containing rabbit anti-CB1R (1:500) and mouse anti-NET (1:1000) in 0.1%BSA in 0.1M TS. The NET antibody was visualized using immunoperoxidase detection by incubating sections in biotinylated donkey anti-mouse IgG (1:400, Jackson ImmunoResearch Laboratories) followed by avidin-biotin complex (Vector Laboratories, Burlingame, CA). Then, the sections reacted with 22mg of 3-3' diaminobenzidine (DAB) (Sigma-Aldrich) containing 0.05% hydrogen peroxide for 15 min. For immunogold detection of CB1R, sections were then incubated in ultrasmall gold-conjugated goat anti-rabbit IgG (1:50, Electron Microscopy Sciences) in 0.8% BSA in 0.01M PBS containing 0.1% fish gelatin (Amerhsam Corp., Amerhsam, England), for 2 hours. Sections were rinsed in same buffer and then rinsed in 0.01M PBS and incubated in 2% glutaraldehyde (Electron Microscopy Sciences) in 0.01M PBS for 10 min followed by washes in 0.01M PBS and 0.2M sodium citrate buffer (pH 7.4). A silver enhancemente kit (Amersham Corp.) was used for silver intensification of the gold particles. Following intensification, tissue was rinsed in 0.1M PB and incubated in 2% osmium tetroxide in 0.1M PB for 1 hour, washed in 0.1M PB, dehydrated and flat embedded in Epon 812 (Electron Microscopy Sciences). The reverse labeling was performed in which CB1R was visualized by immunoperoxidase detection by using biotinylated donkey anti-rabbit (1:400, Jackson ImmunoResearch Laboratories) and immunogold detection of NET was visualized by ultrasmall gold-conjugated goat anti-mouse IgG (1:50, Electron Microscopy Sciences). Thin sections of 74nm in thickness from the mid-ventral shell of the Acb were cut using diamond knife and collected on copper mesh grids.

Controls

For western blot analysis, in order to minimize differences in the areas excised for protein extraction, the same investigator conducted the tissue dissection. To minimize protein loading errors, all gels ran were loaded by the same person.

For immunohistochemical experiments, to control for specificity of the secondary antibodies, controls were run in parallel, in which the primary antisera was omitted. Sections processed in the absence of primary antibody did not exhibit immunoreactivity. To evaluate cross-reactivity of labeling of the primary antiserum by secondary antisera, some sections were processed for dual labeling with omission of one of the primary antisera. To assure that DBH and NET stained the same profiles, dual immunofluorescence for DBH and NET was performed in tissue sections containing the Acb as described before (S4).

Data analysis

Western blot—Blots were scanned into a PC computer and band intensities were quantified using Kodak Molecular Imaging Software (Version 4.5, Carestream Health Inc., Rochester, NY). Intensity of bands for the adrenergic receptor proteins was normalized to that of β-actin in the same sample. Average intensity of bands for acute control tissues was arbitrarily set at 1. Statistical analysis was performed using SPSS 16.0 Graduate Student Version. Statistical analysis of data from the dose response study was conducted using a one-way ANOVA followed by *post-hoc* Bonferroni (with significance set at $p<0.05$). For the analysis of the effects of acute, chronic and abstinence, a 2×3 ANOVA crossing drug treatment (vehicle and drug) with treatment duration (acute, chronic and abstinence) was conducted. When a significant interaction was observed between the two factors, simple effects tests were conducted and a Bonferronni correction was applied. The results are expressed as fold change from vehicle group + standard error (SEM).

Light microscopy—Slides with single labeled sections were visualized using a Leica DMRBE microscope (Wetzlar, Germany), and images were acquired using SPOT Advanced software (Diagnostics Instruments, Inc., Sterling Heights, MI). Figures were then assembled and adjusted for brightness and contrast in Adobe Photoshop CS2. Schematics showing the distribution of CB1R and DBH immunoreactivity are represented on coronal diagrams (from +2.7mm – +1.0mm from bregma) from the Rat Brain Atlas (Paxinos & Watson, 1997) by direct visualization of slides using a light microscope. Schematics were subsequent assembled in Adobe Photoshop CS2.

Dual immunofluorescence—For immunofluorescence, sections were visualized using a confocal microscope (Zeiss LSM 510 Meta, Carl Zeiss Inc., Thornwood, NY). Z-stacks from areas with dual labeling were collected and analyzed; single optical planes were analyzed individually for distribution and co-localization of the two markers throughout the thickness of the section. The data presented represent projections of six to nine single optical planes except for dual fluorescence in the NTS and CB1R and MAP2 pictures where a single plane from z-stack is shown. Digital images were obtained and imported using the LSM 5 image browser. Figures were assembled and adjusted for brightness and contrast in Adobe Photoshop CS2.

Electron microscopy—For ultrastructural analysis, at least 15 grids containing 4 to 8 thin sections (74nm of thickness) each were collected from at least three plastic-embedded sections of the mid-ventral shell of the Acb from each animal. Thin sections were viewed using a Morgagni 268 digital electron microscope (FEI Company, Hillsboro, OR); initially at low magnification to ensure that background labeling in the neuropil, deemed spurious, was not commonly encountered, then at higher magnification to verify adequate cellular morphology. For quantification, electron micrographs from thin sections of three animals that showed optimal preservation of ultrastructural morphology were taken at different magnifications, usually at 11,000× and then at 14,000 to 22,000× for better resolution of the structures analyzed. Figures presented were assembled and adjusted for brightness and contrast in Adobe Photoshop CS2. Selective gold-silver-labeled profiles were identified by

the presence of at least two gold particles within a cellular compartment. The criteria of a minimum of 2 gold particles as indicative of positive immunolabeling is based on the fact that one gold particle could occasionally be found in profiles known to lack CB1R or NET immunoreactivity, such as myelin and blood vessels. Immunoperoxidase labeling was regarded as positive when the electron dense precipitate in individual profiles was considerably greater than that seen in other morphologically similar profiles in the neuropil. The cellular elements were identified based on the description of Peters and colleagues (1991). Somata contained a nucleus, Golgi apparatus and smooth endoplasmic reticulum. Proximal dendrites contained endoplasmic reticulum, were postsynaptic to axon terminals and were larger than 0.7 μm in diameter. A terminal was considered to form a synapse if it showed a junctional complex, a restricted zone of parallel membranes with slight enlargement of the intercellular space, and/or associated with postsynaptic thickening. Asymmetric synapses were identified by thick postsynaptic densities (Gray's type I), in contrast, symmetric synapses had thin densities (Gray's type II) both pre- and postsynaptically. The term "undefined" synaptic contact was used to denote parallel membrane association of an axon terminal plasma membrane juxtaposed to that of a dendrite or soma which lacked recognizable membrane specializations in the plane of section analyzed, and with no intervening glial processes. The term "apposition" was also used to denote close parallel membrane associations of axon terminals with other axon terminals and/or dendrites which lacked recognizable specializations but were otherwise not separated by glial processes.

RESULTS

WIN 55,212-2 alters the expression of adrenergic receptors in the Acb

The influence of a cannabinoid agonist on adrenergic receptor expression in the Acb was assessed by Western blot analysis of protein extracts that were obtained from the Acb of animals that received either an acute systemic injection of WIN 55,212-2, repeated systemic injections of WIN 55,212-2 or repeated systemic injections of WIN 55,212-2 followed by a period of abstinence. The region targeted for tissue dissection included the area medial to the anterior commissure (shell and medial core). As reported by others (Rudoy & Van Bockstaele, 2007), protein extracts indicative of α2A-AR could be identified at approximately 45 kDa while proteins indicative of β1-AR migrated to approximately 65 kDa.

Several studies have reported that CB1R agonists have biphasic effects on behavior according to the dose used, with lower doses stimulating locomotion and higher doses inhibiting it (Rodriguez de Fonseca *et al.*, 1998; Drews *et al.*, 2005). Cannabinoids have also been shown to have anxiolytic and anxiogenic effects on animals (Witkin *et al.*, 2005). For the dose response study, a one-way ANOVA analysis demonstrated a significant difference among treatment groups in β1-AR protein expression (p=0.02; $F_{(3,12)}=10.833$) and *post-hoc* comparison tests revealed that acute administration of WIN 55,212-2 induces a decrease in the expression of β1-AR at the concentrations of 1.0 and 3.0 mg/kg (p<0.05) when comparing to vehicle treated animals (Fig. 3A). Conversely, one-way ANOVA analysis revealed no significant difference in α2A-AR protein expression (p=0.271; $F_{(3,14)}=1.49$) demonstrating that none of the concentrations used had an effect on α2A-AR protein levels in the Acb with an acute injection (Fig. 3A). To investigate the effects of repeated administration of WIN 55,212-2, the 3.0 mg/kg concentration was used as it has also been shown that this concentration, but not 1.0 mg/kg, increases extracellular NE in the PFC (Oropeza *et al.*, 2005). In addition, 3.0 mg/kg was shown to induce c-fos expression in the NTS (Jelsing *et al.*, 2009). Worthy of note, the high dose used (7.0 mg/kg) had very pronounced sedative effect on the animals, making this dose not suitable for future studies.

To assess the effects of repeated administration of WIN 55,212-2 in α2A-AR and β1-AR protein expression a two-way ANOVA crossing drug treatment (vehicle and drug) with treatment duration (acute, chronic and abstinence) was conducted (Fig. 3B). With respect to the effects in α2A-AR expression, the analysis revealed a significant interaction between the two factors (p=0.03, $F_{(2,26)}$=4.103). Therefore, simple effects tests comparing vehicle and drug treated animals were conducted for the acute, chronic and abstinence conditions. A Bonferronni correction was applied. No differences on α2A-AR expression were observed with an acute injection of WIN 55,212-2 (3.0mg/kg). However, the mean difference observed in the chronic condition (mean difference=0.42) was significant (p<0.01; $t_{(5)}$=7.09). Similar effects were observed for the abstinence condition (mean difference=0.54; p<0.001; $t_{(11)}$=4.87). This shows that repeated treatment with WIN 55,212-2 (3.0 mg/kg) for 7 days (chronic group) significantly decrease the expression of α2A-AR and that this effect persisted over time as α2A-AR expression levels remained below control levels in the abstinence group. With respect to the effects in β1-AR protein expression, the analysis revealed a significant effect of drug treatment (p<0.001; $F_{(1.32)}$=15.32) and treatment duration (p<0.001; $F_{(2,32)}$=10.67). The effect of treatment condition suggests that subjects given WIN 55,212-2 show a significantly decrease on β1-AR expression comparing to vehicle-treated animals. However, no interaction between the two factors was noted (p=0.353; $F_{(2,21)}$=1.076).

Two-way ANOVA analysis revealed no significant interaction in α2A-AR (p=0.668; $F_{(2,16)}$=0.414) and β1-AR (p=0.29; $F_{(2,18)}$=1.327) protein expression in samples from the cerebellum, an area rich in CB1R and noradrenergic input (data not shown). No significant effect was observed with respect to NET expression after treatment with WIN 55,212-2 (3.0gmg/kg) (p=0.466; $F_{(1,18)}$=0.555) (S5).

Topographic distribution of CB1R in Acb core and shell subregions

The Acb extends for approximately 2.2 mm in the ventral striatum and is composed of a central "core" and a peripheral and medially situated "shell" subregion (Zahm, 1999; van Dongen *et al.*, 2008).To adequately distinguish the neuroanatomical boundaries of the core and shell subregions within the Acb, calbindin immunoreactivity was used as a marker to define these two subregions in adjacent coronal sections. As previously reported (Jongen-Relo *et al.*, 1994; Tan *et al.*, 1999), calbindin immunoreactivity was more prominent in the core and the overlying striatum where it often appeared in cell bodies (Fig. 4B). Our data are consistent with these reports, as calbindin immunoreactivity appeared prominently in the Acb core where peroxidase-labeled cell bodies could be identified immediately adjacent to the anterior commissure and approaching the lateral ventricle dorsally. The distribution of calbindin immunoreactivity along with the anterior commissure and lateral ventricle were used as references to identify the level of Acb and its subregions when analyzing the distribution of CB1R and DBH (Fig. 4A and 4B). The rostro-caudal segment of the Acb was systematically categorized into three levels for the purpose of the analysis; rostral (from +2.7mm to +1.7mm anterior to bregma), middle (from +1.7mm to +1.0mm anterior to bregma) and caudal (from +1.0mm to +0.6mm anterior to bregma), coordinates according to the Paxinos and Watson Rat Brain Atlas (Paxinos & Watson, 1997).

Localization of CB1R in the Acb was consistent with previous reports (Robbe *et al.*, 2001; Pickel *et al.*, 2004; Kearn *et al.*, 2005). Immunoperoxidase and immunofluorescence labeling of CB1R was identified in long, beaded processes (Fig. 4C, 5A and B) consistent with axonal profiles and punctate deposits that were more consistent with a postsynaptic distribution (Fig. 5A). For simplicity, only CB1R processes are represented on the schematic illustrations (Fig. 6). CB1R immunoreactive (CB1R-ir) processes were found throughout the rostro-caudal extent of the Acb but with a differential distribution within the shell and core subregions. CB1R-ir shifted from dorsal to ventral aspects of the shell as the Acb progresses

caudally. However, in the caudal third division of the Acb, CB1R-ir was more prominent within the Acb core subregion (up to +1.0mm from bregma) with little immunoreactivity in the shell (Fig. 4F). Clusters of CB1R-ir processes were particularly evident in the mid-ventral shell and in the core at caudal levels (Fig. 4E and F, 5B). CB1R labeling was seen in long processes running either medially or ventrally. Although not depicted on the schematic illustrations, CB1R was also seen in profiles consistent with somatodendritic profiles (Fig. 5A) as reported by others (Pickel *et al.*, 2004; Kearn *et al.*, 2005; Villares, 2007). To confirm the somatodendritic localization of CB1R in this region, dual immunofluorescence of CB1R and the somatodendritic marker, MAP2, showed dual labeling for both indicating that CB1R is also present postsynaptically (Fig. 5E).

At the ultrastructral level, using immunogold-silver detection method, CB1R was identified both pre- (Fig. 7A) and post-synaptically (Fig. 7B) in cellular profiles. Of 342 CB1R-ir cellular profiles examined, 55% (189/342) of CB1R-ir was found in axon terminals and 45% (153/342) in dendrites, Pickel and colleagues (2004) reported similar values, 59% in terminals and 41% in dendrites. Similar values were obtained when CB1R was visualized using immunoperoxidase detection. Immunocytochemical labeling for CB1R-ir was identified along the plasma membrane of axon terminals as well as within the axoplasm (Fig. 7). Axon terminals that exhibited CB1R-ir were unmyelinated and contained synaptic vesicles that were heterogeneous in nature. CB1R-ir dendrites contained mitochondria and endoplasmic reticulum and were post-synaptic mainly to unlabeled terminals. Of the axon terminals exhibiting CB1R-ir, synaptic specializations were characterized as symmetric or asymmetric. Semi-quantitative analysis showed that out of 189 profiles counted, 17% (32/189) formed symmetric synapses while 20% (37/189) formed asymmetric synapses (Fig. 7A). The remaining profiles did not form clearly recognizable synaptic specializations in the plane of section analyzed to be accurately classified.

Topographic distribution of DBH in Acb core and shell subregions

Although distributed throughout the entire rostro-caudal extent of the Acb, DBH-ir fibers also showed a topographic distribution (Fig. 4 and 6). DBH-ir was found both in the shell and core of the Acb except for more caudal levels (+1.0mm to +0.7mm from bregma) where DBH-ir was found mainly in the shell (Fig. 4H). This level corresponded to the area of the Acb with the highest density of DBH-ir where abundant, beaded and tortuous DBH-ir fibers were seen. The density of DBH-ir fibers decreased towards more rostral levels, with few fibers being detected at the most rostral level (+2.7mm from bregma). Regions of high overlap between DBH- and CB1R-ir included the ventromedial shell at mid levels of the Acb (Fig. 6, panels 1.7 and 1.6mm).

Ultrastructural analysis of noradrenergic terminals was also assessed by electron microscopy. NET was used as a marker to detect noradrenergic axon terminals and did not compromise the ultrastructural preservation of the neuropil. In order to assure that NET labeled the same profiles as DBH, dual immunofluorescence was performed showing co-localization of both markers in the same profiles (S4). At the ultrastructural level, NET was detected only in axon terminals. The peroxidase reaction resulted in a difuse labeling within the terminals with more intense labeling adjacent to the plasma membrane (arrows in Fig. 7) while immunogold-silver particles were found mainly in the cytoplasm, as reported by Miner and colleagues (2003) in the PFC. Detection of NET with immunogold-silver particles allowed better characterization of the synaptic specialization of these axon terminals in 31% of the terminals analyzed (47/153). NET was found to form mainly symmetric synapses (31 of 47, 66%), in accordance with studies in the PFC (Miner *et al.*, 2003), while asymmetric synapses were found in 34% (16/47).

Immunofluorescence microscopy shows that CB1R and DBH overlap in both core and shell subregions of the Acb

Dual-immunofluorescence for CB1R and DBH was conducted in the same section of tissue to determine whether noradrenergic afferents exhibit CB1R immunoreactivity. Both CB1R- and DBH-ir were found in beaded and tortuous processes (Fig. 5). The beaded morphology was more evident within the DBH-ir fibers (Fig. 5B and C). The distribution of CB1R and DBH-ir in the Acb was in concordance with the data obtained from single labeling described above. Although CB1R-ir was often found in areas containing noradrenergic fibers, rarely were noradrenergic fibers positive for CB1R. However, in these areas of overlap, CB1R and DBH-ir appeared to converge on common structures as the processes appeared to delineate cell bodies of neurons in the Acb (double arrows in Fig. 5B), suggesting that noradrenergic fibers and fibers containing CB1R may be converging on common neurons.

Noradrenergic afferents to the shell of the Acb show a low frequency of co-existence with CB1R

The dual immunofluorescence data suggested multiple sites of interaction between CB1R and noradrenergic afferents that could only be fully resolved using ultrastructural analysis. The mid-ventral shell of the Acb was the area sampled for EM analysis based on the light microscopic data showing significant overlap in this area (Fig. 6). NET was detected using immunoperoxidase detection while CB1R was localized using immunogold-silver deposits (Fig. 7). In the area sampled, CB1R and noradrenergic terminals were found to physically interact in two ways. Some noradrenergic terminals were found to have CB1R and some were found to be apposed to unlabeled profiles containing CB1R. More specifically, 7.7% (9/113) of all NET immunoreactive (NET-ir) axon terminals contained CB1R immunogold silver particles, while 4.8% (9/189) of all CB1R containing axon terminals were found in NET-ir axon terminals (Fig. 7F). With respect to the apposed labeling, 6.2% (7/113) of all NET-ir axon terminals were apposed to profiles containing CB1R immunogold silver particles (Fig. 7D). Conversely, 1.6% of all CB1R containing axon terminals were apposed to NET-ir axon terminals, while 2.6% of all CB1R containing dendrites were apposed to NET-ir axon terminals. In regions of apposition, no synaptic specialization of the CB1R containing terminals was recognizable in the cross section analyzed.

CB1R are located to noradrenergic neurons in the NTS

Since the cannabinoid agonist was administered systemically, the effects of WIN 55,212-2 on the expression of AR in the Acb could also be due to its actions on CB1R localized to noradrenergic nuclei projecting to the Acb, i.e. the NTS. To assess this, dual immunofluorescence for CB1R and DBH was performed in tissue sections containing the NTS. DBH-ir was found diffusely in cell bodies as well as in processes resembling dendrites (Fig. 5D). CB1R-ir exhibited a punctate distribution and co-localized to the cytoplasm of noradrenergic neurons (positive for DBH) as well as non-noradrenergic neurons (lacking DBH-ir). Some of DBH-labeled neurons lacked CB1R-ir.

DISCUSSION

The present study demonstrates that systemic administration of a cannabinoid agonist alters the expression of ARs in a key limbic forebrain region related to motivated behaviors. Light and ultrastructural microscopy studies indicate several potential cellular sites for interaction between the two systems that include co-existence in common axon terminals, serial modulation by convergence of separately labeled axon terminals on common postsynaptic targets and indirect effects on noradrenergic brainstem perikarya that provide afferent input to the Acb.

Methodological considerations

The present study analyzed the expression of AR in the Acb following treatment with WIN 55,212-2 or vehicle. The Acb can be divided into core and shell subregions. At more rostral levels, the two regions can be easily microdissected but at more caudal levels, the core subregion completely surrounds the anterior commissure while the shell subregion surrounds it ventrally. To avoid dissecting the anterior commissure, we oriented our micropunches to target the Acb medial to the anterior commissure, leaving out the core that sits lateral to it and part of the ventrolateral shell from the dissection. Since micropunches of the Acb were used for the quantification of the ARs, the exact area where these changes occurred (shell vs core subregions, rostral vs caudal) cannot be established. Also, whether the changes observed are due to a decrease in both pre- and post-synaptic receptors cannot be defined.

A potential limitation known to be associated with the pre-embedding immunolabeling technique is attributed to penetration of immunoreagents in thick Vibratome sections (Chan *et al.*, 1990). To circumvent this caveat, analysis of ultrathin sections was carried out exclusively on sections near the tissue/plastic interface where penetration is maximal. Limitations associated with the specificity of immunogold labeling were overcome by quantifying only the profiles containing two or more immunogold-silver particles. This may contribute to an underestimation of actual cellular relationships. However, this approach minimized the reporting of potential spurious gold labeling.

AR changes in the Acb following CB1R agonist treatment

To our knowledge, we are the first to report a change in adrenergic receptor expression in the Acb following exposure to systemic administration of the synthetic cannabinoid agonist WIN 55,212-2. Our results demonstrate a decrease in β1- and α2A-AR protein expression in the Acb following acute and/or chronic exposure. A decrease in protein expression levels may be related to downregulation of the receptor as adrenergic receptors, which belong to the G protein-coupled receptor superfamily (GPCR), are known to desensitize, internalize and downregulate their expression following binding of an agonist (Heck & Bylund, 1997; Dunigan *et al.*, 2002). Because desensitization does not seem to depend on protein degradation (as removal of agonist rapidly restores receptor function) (Hein & Kobilka, 1995) no differences in total receptor protein are expected during desensitization. In contrast, downregulation of GPCRs can be defined as a loss of total cellular binding activity or decrease in receptor density (Barturen & Garcia-Sevilla, 1992; Hein & Kobilka, 1995; Heck & Bylund, 1997). Mechanisms for downregulation may include protein degradation, destabilization of the receptor mRNA or repression of gene transcription.

We have previously reported that acute and chronic systemic administration of WIN 55,212-2 is capable of increasing NE release in the PFC with concomitant activation of c-fos activation in brainstem noradrenergic neurons (Oropeza *et al.*, 2005; Page *et al.*, 2007). In addition, others have shown that WIN 55,212-2 (3.0mg/kg) is able to induce c-fos expression in the NTS (Jelsing *et al.*, 2009). It is tempting to speculate that the downregulation of AR in the Acb following WIN 55,212-2 may occur due to an increase in NE release in the Acb. The fact that NET expression in the Acb is not affected by WIN 55,212-2 administration, suggests that the reuptake of NE by this transporter remains constant although binding tests should be performed to confirm this. We have recently described a decrease in β1-AR levels in the PFC after chronic treatment with WIN 55,212-2 with no changes in the levels of α2A-AR (Reyes *et al.*, 2009). The distinct effect of WIN 55,212-2 on the levels of ARs in the PFC and Acb may account for the anatomical and functional differences between the two areas. Anatomically, the PFC receives its noradrenergic input solely from the LC while the Acb is innervated mainly by the NTS

(Delfs *et al.*, 1998; Olson *et al.*, 2006). The present study, therefore, by assessing noradrenergic afferents to the Acb, provides information regarding the interaction of the cannabinoid system with limbic-forebrain projections originating specifically from the NTS. Also, the subcellular localization of the AR in the Acb is not known but they are found to be both pre- and post-synaptic in other brain regions, such as the PFC (MacDonald *et al.*, 1997; Ramos & Arnsten, 2007; Wang *et al.*, 2007). The localization of AR with CB1R is being analyzed and, based on previous studies showing preferential presynaptic localization of α2-AR (Flugge *et al.*, 2004), we hypothesize that axon terminals in the Acb expressing α2-AR will be apposed to terminals containing CB1R. Considering our localization of CB1R in dendrites and the known association of β1-AR receptors with the postsynaptic density protein in other brain regions (Strader *et al.*, 1983; Aoki *et al.*, 1987; Hu *et al.*, 2000), we also anticipate a potential co-localization of β1-AR and CB1R postsynaptically. It has been proposed that activation of CB1R can sequester G-proteins making them unavailable for other GPCRs, such as α2-AR and somatostatin receptor (Vasquez & Lewis, 1999). Whether disruption of these GPCRs signaling can ultimately lead to theirs downregulation has not been addressed yet. Activation of CB1R is also known to lead to changes in membrane potential and to alter the levels of intracellular cAMP (Demuth & Molleman, 2006). cAMP can initiate intracellular pathways that can lead to inhibition of AR synthesis or to destabilization of AR mRNA, contributing to downregulation of the receptor (Kirigiti *et al.*, 2001; Dunigan *et al.*, 2002). In addition, stimulation of CB1R activates protein kinases that could participate in the regulation of gene expression (Piomelli, 2003).

CB1R and DBH are topographically distributed within the Acb

Our data are in agreement with others with regard to the presence of noradrenergic terminals and CB1R immunoreactivity in the Acb (Berridge *et al.*, 1997; Delfs *et al.*, 1998; Tsou *et al.*, 1998; Robbe *et al.*, 2001). However, the present study adds a detailed analysis of the distribution of CB1R-ir not provided in these studies. Robbe and colleagues (2001) identified CB1R-ir in large, poorly branched fibers exhibiting intensely immunostained varicosities that were localized mostly to the core subregion of the Acb. We report the same type of immunostaining for CB1R but we provide new data showing that CB1R is also found in the shell subregion. Our analysis shows that CB1R-ir is not uniform throughout the Acb. CB1R-ir is mainly found in the core in the caudal third of the Acb and is found in the remaining two thirds of the nucleus in the shell subregion. Hence, CB1R-ir seems to be more abundant in the shell. Careful analysis by light microscopy of CB1R-ir in both the core and the shell subregions did not reveal major differences in the immunostaining pattern between the subregions suggesting that CB1R may function similarly in both the shell and core. The distribution of DBH-ir in the Acb presented in this study is in agreement with previous studies (Berridge *et al.*, 1997; Delfs *et al.*, 1998). More specifically, DBH-ir was reported to be more evident in the shell at caudal levels but it was also found at more rostral levels, both in the shell and in the core.

In summary, our mapping of CB1R- and DBH-ir in the Acb shows an interesting topographic distribution of the two markers. CB1R and DBH were shown to have an uneven distribution throughout the nucleus. This fact may be relevant for the anatomic and functional heterogeneity proposed for the Acb (Zahm, 1999). Anatomical and behavioral studies support a rostro-caudal gradient for appetitive vs. aversive behaviors (Reynolds & Berridge, 2001, 2002, 2003). These studies suggest that the rostral shell is important for appetitive/hedonic behaviors whereas the caudal shell is important for aversive/fear behaviors and that GABAergic and glutamatergic transmission (through GABA$_A$ and AMPA receptors) is involved. Modulation of GABAergic and glutamatergic transmission in the intermediate shell produces combined positive and negative motivational effects. Whether the overlapping region of DBH and CB1R immunoreactivities described in the

present study correlates with these behaviors cannot be established. However, our ultrastructural analysis of the middle third of the shell subregion, localized CB1R to terminals forming symmetric (inhibitory) and asymmetric (excitatory) synapses, suggesting that activation of CB1R can modulate inhibitory and excitatory input in the Acb and therefore modulate behavior. In addition, previous studies have shown that cannabinoids are able to inhibit glutamate and GABA transmission in the Acb (Hoffman & Lupica, 2001; Manzoni & Bockaert, 2001; Robbe *et al.*, 2001; Hoffman *et al.*, 2003) mainly through a pre-synaptic mechanism. Future studies should also address whether the presence of noradrenergic fibers in this specific region is important for the modulation of the abovementioned behaviors.

Subcellular localization of CB1R in the Acb

The CB1R subcellular distribution in the shell of the Acb analyzed in the present study by electron microscopy is agreement with previous studies but also shows some differences (Pickel *et al.*, 2004; Matyas *et al.*, 2006). Discrepancies in anatomical studies may arise from multiple factors. For example, the region of the Acb analyzed may differ from study to study. As shown in the present study, the distribution of both CB1R and noradrenergic fibers varies considerably throughout the nucleus and sampling differences between laboratories may lead to different results. In the present study, the area selected for ultrastructural analysis was restricted to the mid-ventral shell due to the higher incidence of overlap between CB1R- and DBH-ir observed by light and fluorescence microscopy. In addition, different criteria were used to quantify profiles that exhibited CB1R immunoreactivity. In the present study, only profiles containing two or more gold particles were included in the semi-quantitative analysis whereas other groups (Pickel *et al.*, 2004) considered single immunogold-silver profiles as indicative of positive labeling for CB1R. Finally, another difference relates to the type of synapses formed by terminals containing CB1R. Mátyás and colleagues (2006) showed that all single-labeled CB1R-containing axon terminals and dual-labeled CB1R and GABA axon terminals formed exclusively symmetric synapses. On the other hand, Pickel and colleagues (2004) reported that 42% of the CB1R-labeled axon terminals formed asymmetric synapses while only 7% formed symmetric synapses. In the present study, a similar number of terminals formed symmetric and asymmetric synapses, although more than 60% of the profiles exhibited synaptic specifications that could not be unequivocally established in the plane of section analyzed. Nevertheless, as mentioned before, cannabinoids were found to affect both glutamate and GABA transmission in the Acb (Manzoni & Bockaert, 2001; Robbe *et al.*, 2001). Therefore, the localization of CB1R in terminals forming symmetric and asymmetric synapses, in the present study, is consistent with this.

As reported by Pickel and colleagues (2004), the present study shows immunolabeling for CB1R in somatodendritc profiles in the Acb. This is an interesting finding as cannabinoid actions are thought to be mainly pre-synaptic. However, there is evidence for self-inhibition of cortical interneurons by cannabinoids in an autocrine way, where cannabinoids are synthesized post-synaptic and activate nearby CB1R (Piomelli, 2003; Bacci *et al.*, 2004). Moreover, the fact that fatty acid amide hydrolase (one of the enzymes responsible for degradation of endocannabinoids) is located mainly in cell bodies and dendrites (Egertova *et al.*, 2003; Piomelli, 2003) may suggest that cannabinoids might be able to act post-synaptically. Nevertheless, whether CB1R located post-synaptically in the Acb are functional and activating intracellular pathways was not investigated in the present study and warrants further investigation..

Anatomical data shows interaction between CB1R and DBH

Our anatomical data show multiple sites for interaction between the cannabinoid and noradrenergic systems in the Acb and the NTS (Fig. 8). CB1R was found in noradrenergic terminals, in unlabeled terminals apposed to noradrenergic terminals and in dendrites in the Acb as well as in noradrenergic and non-noradrenergic neurons of the NTS (Fig. 8.1). Based on our anatomical data, we proposed four potential mechanisms by which WIN 55,212-2 is modulating AR expression. WIN 55,212-2 may be modulating the levels of AR directly by activating CB1R present in profiles that express AR (dendrites or axon terminals) (Fig. 8.2). WIN 55,212-2 can also act on CB1R present in noradrenergic terminals (Fig. 8.2) modulating the release of NE. Continued agonist-activation of AR by NE can lead to receptor downregulation (Hein & Kobilka, 1995; Heck & Bylund, 1997). A third intra-accumbal mechanism may account for WIN 55,212-2 modulation of AR. The majority of CB1R was found in unlabeled profiles. The nature of these profiles is unknown, but activation of CB1R by WIN 55,212-2 may contribute to modulation of these profiles transmission with consequent effects on noradrenergic terminals and profiles containing AR (Fig. 8.3). Ultimately, WIN 55,212-2 may be acting on CB1R present in the NTS, increasing the noradrenergic input to the Acb (Fig. 8.4). In fact, WIN 55,212-2 administration was shown to induce c-fos activation in the NTS (Jelsing *et al.*, 2009). However, whether this neuronal activation increases NE release in the Acb remains to be elucidated.

Functional implications

Convergent studies in the literature suggest that cannabinoids may play a role in several neuropsychiatric disorders (Maldonado *et al.*, 2006; Leweke & Koethe, 2008; Moreira & Lutz, 2008), such as depression or schizophrenia. Interestingly, the CB1R antagonist rimonabant was withdrawn due to an unacceptably high incidence of neuropsychiatric side effects (Nissen *et al.*, 2008; Sanofi-Aventis), while CB1R agonist has been shown to alleviate depressive-like behaviors in animal models (Gobbi *et al.*, 2005; Hill & Gorzalka, 2005b). Moreover, Gobbi and colleagues (2005) showed that increased levels of anandamide evoked an increase in noradrenergic neuron activity in the LC. This is supported by previous work from our laboratory, showing that administration of a synthetic cannabinoid is able to activate the LC with increased levels of NE in the PFC (Oropeza *et al.*, 2005; Page *et al.*, 2007). The present study adds to this data, since the decrease in α2A-AR expression may account for the assumed increase in NE in the Acb, as α2A-AR seems to function as autoreceptors by inhibiting NE release from the pre-synaptic terminal (Kable *et al.*, 2000). In fact, local administration of α2-AR agonists in the Acb has been shown to reduce the efflux of NE measured by microdialysis, while administration of antagonists of α2-AR increased the release of NE (Aono *et al.*, 2007). Moreover, downregulation of β1-AR can be seen as an adaptive mechanism to an increase in synaptic NE. Although activation of α2-AR can decrease dopamine release in other brain regions, such as the PFC and hippocampus (Guiard *et al.*, 2008; Jentsch *et al.*, 2008) this does not seem to be the case in the Acb. Ihalainen and colleagues have shown that administration of an α2-AR agonist would decrease dopamine in the Acb when administered systemically but not when it was locally administered (Ihalainen & Tanila, 2004). This supports the idea that α2-AR may localize mainly to noradrenergic terminals in the Acb. Therefore, the impact of chronic WIN 55,212-2 on α2-AR levels in the Acb seems to be selective for noradrenergic terminals. Since NE is an important target for the treatment of depression (Heninger *et al.*, 1996; Nutt, 2002), it is tempting to speculate that cannabinoids may impact mood and motivation related behaviors by activating limbic forebrain noradrenergic circuits.

Supplementary Material

Refer to Web version on PubMed Central for supplementary material.

Acknowledgments

Abbreviations

Acb	Nucleus accumbens
AR	Adrenergic receptor
CB1R	Cannabinoid receptor type 1
DBH	Dopamine beta hydroxylase
GPCR	G protein-coupled receptor
LC	Locus coeruleus
MAP2	Microtubule associated protein 2
NE	Norepinephrine
NET	Norepinephrine transporter
NTS	Nucleus of the solitary tract
PFC	Prefrontal cortex

References

Anand A, Charney DS. Norepinephrine dysfunction in depression. J. Clin. Psychiatry. 2000; 61(Suppl 10):16–24. [PubMed: 10910013]

Aoki C, Joh TH, Pickel VM. Ultrastructural localization of beta-adrenergic receptor-like immunoreactivity in the cortex and neostriatum of rat brain. Brain Res. 1987; 437:264–282. [PubMed: 2829995]

Aono Y, Saigusa T, Watanabe S, Iwakami T, Mizoguchi N, Ikeda H, Ishige K, Tomiyama K, Oi Y, Ueda K, Rausch WD, Waddington JL, Ito Y, Koshikawa N, Cools AR. Role of alpha adrenoceptors in the nucleus accumbens in the control of accumbal noradrenaline efflux: A microdialysis study with freely moving rats. J. Neural Transm. 2007; 114:1135–1142. [PubMed: 17533511]

Aston-Jones G, Chiang C, Alexinsky T. Discharge of noradrenergic locus coeruleus neurons in behaving rats and monkeys suggests a role in vigilance. Prog. Brain Res. 1991; 88:501–520. [PubMed: 1813931]

Bacci A, Huguenard JR, Prince DA. Long-lasting self-inhibition of neocortical interneurons mediated by endocannabinoids. Nature. 2004; 431:312–316. [PubMed: 15372034]

Barturen F, Garcia-Sevilla JA. Long term treatment with desipramine increases the turnover of alpha 2-adrenoceptors in the rat brain. Mol. Pharmacol. 1992; 42:846–855. [PubMed: 1359398]

Berridge CW, Stratford TL, Foote SL, Kelley AE. Distribution of dopamine beta-hydroxylase-like immunoreactive fibers within the shell subregion of the nucleus accumbens. Synapse. 1997; 27:230–241. [PubMed: 9329158]

Bodor AL, Katona I, Nyiri G, Mackie K, Ledent C, Hajos N, Freund TF. Endocannabinoid signaling in rat somatosensory cortex: Laminar differences and involvement of specific interneuron types. J. Neurosci. 2005; 25:6845–6856. [PubMed: 16033894]

Callado LF, Meana JJ, Grijalba B, Pazos A, Sastre M, Garcia-Sevilla JA. Selective increase of alpha2A-adrenoceptor agonist binding sites in brains of depressed suicide victims. J. Neurochem. 1998; 70:1114–1123. [PubMed: 9489732]

Chan J, Aoki C, Pickel VM. Optimization of differential immunogold-silver and peroxidase labeling with maintenance of ultrastructure in brain sections before plastic embedding. J. Neurosci. Methods. 1990; 33:113–127. [PubMed: 1977960]

Daniel H, Crepel F. Control of ca(2+) influx by cannabinoid and metabotropic glutamate receptors in rat cerebellar cortex requires K(+) channels. J. Physiol. 2001; 537:793–800. [PubMed: 11744755]

De Paermentier F, Mauger JM, Lowther S, Crompton MR, Katona CL, Horton RW. Brain alpha-adrenoceptors in depressed suicides. Brain Res. 1997; 757:60–68. [PubMed: 9200499]

De Paermentier F, Cheetham SC, Crompton MR, Katona CL, Horton RW. Brain beta-adrenoceptor binding sites in depressed suicide victims: Effects of antidepressant treatment. Psychopharmacology (Berl). 1991; 105:283–288. [PubMed: 1686657]

De Paermentier F, Cheetham SC, Crompton MR, Katona CL, Horton RW. Brain beta-adrenoceptor binding sites in antidepressant-free depressed suicide victims. Brain Res. 1990; 525:71–77. [PubMed: 2173963]

Delfs JM, Zhu Y, Druhan JP, Aston-Jones GS. Origin of noradrenergic afferents to the shell subregion of the nucleus accumbens: Anterograde and retrograde tract-tracing studies in the rat. Brain Res. 1998; 806:127–140. [PubMed: 9739125]

Demuth DG, Molleman A. Cannabinoid signalling. Life Sci. 2006; 78:549–563. [PubMed: 16109430]

Di Chiara G. Nucleus accumbens shell and core dopamine: Differential role in behavior and addiction. Behav. Brain Res. 2002; 137:75–114. [PubMed: 12445717]

Drews E, Schneider M, Koch M. Effects of the cannabinoid receptor agonist WIN 55,212-2 on operant behavior and locomotor activity in rats. Pharmacol. Biochem. Behav. 2005; 80:145–150. [PubMed: 15652390]

Dunigan CD, Hoang Q, Curran PK, Fishman PH. Complexity of agonist- and cyclic AMP-mediated downregulation of the human beta 1-adrenergic receptor: Role of internalization, degradation, and mRNA destabilization. Biochemistry. 2002; 41:8019–8030. [PubMed: 12069593]

Egertova M, Cravatt BF, Elphick MR. Comparative analysis of fatty acid amide hydrolase and cb(1) cannabinoid receptor expression in the mouse brain: Evidence of a widespread role for fatty acid amide hydrolase in regulation of endocannabinoid signaling. Neuroscience. 2003; 119:481–496. [PubMed: 12770562]

Flugge G, Van Kampen M, Mijnster MJ. Perturbations in brain monoamine systems during stress. Cell Tissue Res. 2004; 315:1–14. [PubMed: 14579145]

Fox KM, Sterling RC, Van Bockstaele EJ. Cannabinoids and novelty investigation: Influence of age and duration of exposure. Behav. Brain Res. 2009; 196:248–253. [PubMed: 18951925]

Gerdeman G, Lovinger DM. CB1 cannabinoid receptor inhibits synaptic release of glutamate in rat dorsolateral striatum. J. Neurophysiol. 2001; 85:468–471. [PubMed: 11152748]

Gobbi G, Bambico FR, Mangieri R, Bortolato M, Campolongo P, Solinas M, Cassano T, Morgese MG, Debonnel G, Duranti A, Tontini A, Tarzia G, Mor M, Trezza V, Goldberg SR, Cuomo V, Piomelli D. Antidepressant-like activity and modulation of brain monoaminergic transmission by blockade of anandamide hydrolysis. Proc. Natl. Acad. Sci. U. S. A. 2005; 102:18620–18625. [PubMed: 16352709]

Guiard BP, El Mansari M, Blier P. Cross-talk between dopaminergic and noradrenergic systems in the rat ventral tegmental area, locus ceruleus, and dorsal hippocampus. Mol. Pharmacol. 2008; 74:1463–1475. [PubMed: 18703671]

Heck DA, Bylund DB. Mechanism of down-regulation of alpha-2 adrenergic receptor subtypes. J. Pharmacol. Exp. Ther. 1997; 282:1219–1227. [PubMed: 9316829]

Hein L, Kobilka BK. Adrenergic receptor signal transduction and regulation. Neuropharmacology. 1995; 34:357–366. [PubMed: 7566466]

Heninger GR, Delgado PL, Charney DS. The revised monoamine theory of depression: A modulatory role for monoamines, based on new findings from monoamine depletion experiments in humans. Pharmacopsychiatry. 1996; 29:2–11. [PubMed: 8852528]

Hill MN, Gorzalka BB. Is there a role for the endocannabinoid system in the etiology and treatment of melancholic depression? Behav. Pharmacol. 2005a; 16:333–352. [PubMed: 16148438]

Hill MN, Gorzalka BB. Pharmacological enhancement of cannabinoid CB1 receptor activity elicits an antidepressant-like response in the rat forced swim test. Eur. Neuropsychopharmacol. 2005b; 15:593–599. [PubMed: 15916883]

Hoffman AF, Oz M, Caulder T, Lupica CR. Functional tolerance and blockade of long-term depression at synapses in the nucleus accumbens after chronic cannabinoid exposure. J. Neurosci. 2003; 23:4815–4820. [PubMed: 12832502]

Hoffman AF, Lupica CR. Direct actions of cannabinoids on synaptic transmission in the nucleus accumbens: A comparison with opioids. J. Neurophysiol. 2001; 85:72–83. [PubMed: 11152707]

Hoffman AF, Lupica CR. Mechanisms of cannabinoid inhibition of GABA(A) synaptic transmission in the hippocampus. J. Neurosci. 2000; 20:2470–2479. [PubMed: 10729327]

Hohmann AG, Herkenham M. Localization of cannabinoid CB(1) receptor mRNA in neuronal subpopulations of rat striatum: A double-label in situ hybridization study. Synapse. 2000; 37:71–80. [PubMed: 10842353]

Hu LA, Tang Y, Miller WE, Cong M, Lau AG, Lefkowitz RJ, Hall RA. Beta 1-adrenergic receptor association with PSD-95. inhibition of receptor internalization and facilitation of beta 1-adrenergic receptor interaction with N-methyl-D-aspartate receptors. J. Biol. Chem. 2000; 275:38659–38666. [PubMed: 10995758]

Hurley MJ, Mash DC, Jenner P. Expression of cannabinoid CB1 receptor mRNA in basal ganglia of normal and parkinsonian human brain. J. Neural Transm. 2003; 110:1279–1288. [PubMed: 14628192]

Ihalainen JA, Tanila H. In vivo regulation of dopamine and noradrenaline release by alpha2A-adrenoceptors in the mouse nucleus accumbens. J. Neurochem. 2004; 91:49–56. [PubMed: 15379886]

Jelsing J, Galzin AM, Guillot E, Pruniaux MP, Larsen PJ, Vrang N. Localization and phenotypic characterization of brainstem neurons activated by rimonabant and WIN55,212-2. Brain Res. Bull. 2009; 78:202–210. [PubMed: 19038314]

Jentsch JD, Sanchez D, Elsworth JD, Roth RH. Clonidine and guanfacine attenuate phencyclidine-induced dopamine overflow in rat prefrontal cortex: Mediating influence of the alpha-2A adrenoceptor subtype. Brain Res. 2008; 1246:41–46. [PubMed: 18977208]

Jongen-Relo AL, Voorn P, Groenewegen HJ. Immunohistochemical characterization of the shell and core territories of the nucleus accumbens in the rat. Eur. J. Neurosci. 1994; 6:1255–1264. [PubMed: 7526940]

Kable JW, Murrin LC, Bylund DB. In vivo gene modification elucidates subtype-specific functions of alpha(2)-adrenergic receptors. J. Pharmacol. Exp. Ther. 2000; 293:1–7. [PubMed: 10734146]

Kearn CS, Blake-Palmer K, Daniel E, Mackie K, Glass M. Concurrent stimulation of cannabinoid CB1 and dopamine D2 receptors enhances heterodimer formation: A mechanism for receptor cross-talk? Mol. Pharmacol. 2005; 67:1697–1704. [PubMed: 15710746]

Kirigiti P, Bai Y, Yang YF, Li X, Li B, Brewer G, Machida CA. Agonist-mediated down-regulation of rat beta1-adrenergic receptor transcripts: Role of potential post-transcriptional degradation factors. Mol. Pharmacol. 2001; 60:1308–1324. [PubMed: 11723238]

Leweke FM, Koethe D. Cannabis and psychiatric disorders: It is not only addiction. Addict. Biol. 2008; 13:264–275. [PubMed: 18482435]

MacDonald E, Kobilka BK, Scheinin M. Gene targeting--homing in on alpha 2-adrenoceptor-subtype function. Trends Pharmacol. Sci. 1997; 18:211–219. [PubMed: 9227000]

Mackie K. Distribution of cannabinoid receptors in the central and peripheral nervous system. Handb. Exp. Pharmacol. 2005; (168):299–325. [PubMed: 16596779]

Maldonado R, Valverde O, Berrendero F. Involvement of the endocannabinoid system in drug addiction. Trends Neurosci. 2006; 29:225–232. [PubMed: 16483675]

Manzoni OJ, Bockaert J. Cannabinoids inhibit GABAergic synaptic transmission in mice nucleus accumbens. Eur. J. Pharmacol. 2001; 412:R3–5. [PubMed: 11165232]

Matyas F, Yanovsky Y, Mackie K, Kelsch W, Misgeld U, Freund TF. Subcellular localization of type 1 cannabinoid receptors in the rat basal ganglia. Neuroscience. 2006; 137:337–361. [PubMed: 16289348]

Meana JJ, Barturen F, Garcia-Sevilla JA. Alpha 2-adrenoceptors in the brain of suicide victims: Increased receptor density associated with major depression. Biol. Psychiatry. 1992; 31:471–490. [PubMed: 1349830]

Miner LH, Schroeter S, Blakely RD, Sesack SR. Ultrastructural localization of the norepinephrine transporter in superficial and deep layers of the rat prelimbic prefrontal cortex and its spatial relationship to probable dopamine terminals. J. Comp. Neurol. 2003; 466:478–494. [PubMed: 14566944]

Moranta D, Esteban S, Garcia-Sevilla JA. Chronic treatment and withdrawal of the cannabinoid agonist WIN 55,212-2 modulate the sensitivity of presynaptic receptors involved in the regulation of monoamine syntheses in rat brain. Naunyn Schmiedebergs Arch. Pharmacol. 2009; 379:61–72. [PubMed: 18709357]

Moreira FA, Lutz B. The endocannabinoid system: Emotion, learning and addiction. Addict. Biol. 2008; 13:196–212. [PubMed: 18422832]

Nissen SE, Nicholls SJ, Wolski K, Rodes-Cabau J, Cannon CP, Deanfield JE, Despres JP, Kastelein JJ, Steinhubl SR, Kapadia S, Yasin M, Ruzyllo W, Gaudin C, Job B, Hu B, Bhatt DL, Lincoff AM, Tuzcu EM, STRADIVARIUS Investigators. Effect of rimonabant on progression of atherosclerosis in patients with abdominal obesity and coronary artery disease: The STRADIVARIUS randomized controlled trial. JAMA. 2008; 299:1547–1560. [PubMed: 18387931]

Nutt DJ. The neuropharmacology of serotonin and noradrenaline in depression. Int. Clin. Psychopharmacol. 2002; 17(Suppl 1):S1–12. [PubMed: 12369606]

Olson VG, Heusner CL, Bland RJ, During MJ, Weinshenker D, Palmiter RD. Role of noradrenergic signaling by the nucleus tractus solitarius in mediating opiate reward. Science. 2006; 311:1017–1020. [PubMed: 16484499]

Oropeza VC, Mackie K, Van Bockstaele EJ. Cannabinoid receptors are localized to noradrenergic axon terminals in the rat frontal cortex. Brain Res. 2007; 1127:36–44. [PubMed: 17113043]

Oropeza VC, Page ME, Van Bockstaele EJ. Systemic administration of WIN 55,212-2 increases norepinephrine release in the rat frontal cortex. Brain Res. 2005; 1046:45–54. [PubMed: 15927549]

Page ME, Oropeza VC, Sparks SE, Qian Y, Menko AS, Van Bockstaele EJ. Repeated cannabinoid administration increases indices of noradrenergic activity in rats. Pharmacol. Biochem. Behav. 2007; 86:162–168. [PubMed: 17275893]

Paxinos, G.; Watson, C. The Rat Brain in Stereotaxic Coordinates. Academic Press; New York: 1997.

Peters, AP.; Sl; Webster, HD. The Fine Structure of the NervousSystem. Oxford University Press; New York: 1991.

Pickel VM, Chan J, Kash TL, Rodriguez JJ, MacKie K. Compartment-specific localization of cannabinoid 1 (CB1) and mu-opioid receptors in rat nucleus accumbens. Neuroscience. 2004; 127:101–112. [PubMed: 15219673]

Piomelli D. The molecular logic of endocannabinoid signalling. Nat. Rev. Neurosci. 2003; 4:873–884. [PubMed: 14595399]

Ramos BP, Arnsten AF. Adrenergic pharmacology and cognition: Focus on the prefrontal cortex. Pharmacol. Ther. 2007; 113:523–536. [PubMed: 17303246]

Reyes BAS, Rosario JC, Piana PMT, Van Bockstaele EJ. Cannabinoid Modulation of cortical adrenergic receptors and transporters. J. Neurosci. Res. 2009

Reynolds SM, Berridge KC. Glutamate motivational ensembles in nucleus accumbens: Rostrocaudal shell gradients of fear and feeding. Eur. J. Neurosci. 2003; 17:2187–2200. [PubMed: 12786986]

Reynolds SM, Berridge KC. Positive and negative motivation in nucleus accumbens shell: Bivalent rostrocaudal gradients for GABA-elicited eating, taste "liking"/"disliking" reactions, place preference/avoidance, and fear. J. Neurosci. 2002; 22:7308–7320. [PubMed: 12177226]

Reynolds SM, Berridge KC. Fear and feeding in the nucleus accumbens shell: Rostrocaudal segregation of GABA-elicited defensive behavior versus eating behavior. J. Neurosci. 2001; 21:3261–3270. [PubMed: 11312311]

Robbe D, Alonso G, Duchamp F, Bockaert J, Manzoni OJ. Localization and mechanisms of action of cannabinoid receptors at the glutamatergic synapses of the mouse nucleus accumbens. J. Neurosci. 2001; 21:109–116. [PubMed: 11150326]

Rodriguez de Fonseca F, Del Arco I, Martin-Calderon JL, Gorriti MA, Navarro M. Role of the endogenous cannabinoid system in the regulation of motor activity. Neurobiol. Dis. 1998; 5:483–501. [PubMed: 9974180]

Rudoy CA, Van Bockstaele EJ. Betaxolol, a selective beta(1)-adrenergic receptor antagonist, diminishes anxiety-like behavior during early with drawal from chronic cocaine administration in rats. Prog. Neuropsychopharmacol. Biol. Psychiatry. 2007; 31:1119–1129. [PubMed: 17513029]

Sanofi-Aventis. [accessed online 15 February 2009] Accomplia update. http://en.sanofiaventis.com/investors/events/corporate/2008/081023_investor_update.asp

Shirayama Y, Chaki S. Neurochemistry of the nucleus accumbens and its relevance to depression and antidepressant action in rodents. Curr. Neuropharmacol. 2006; 4:277–291. [PubMed: 18654637]

Siegel JM. Clues to the functions of mammalian sleep. Nature. 2005; 437:1264–1271. [PubMed: 16251951]

Strader CD, Pickel VM, Joh TH, Strohsacker MW, Shorr RG, Lefkowitz RJ, Caron MG. Antibodies to the beta-adrenergic receptor: Attenuation of catecholamine-sensitive adenylate cyclase and demonstration of postsynaptic receptor localization in brain. Proc. Natl. Acad. Sci. U. S. A. 1983; 80:1840–1844. [PubMed: 6300875]

Tan Y, Williams ES, Zahm DS. Calbindin-D 28kD immunofluorescence in ventral mesencephalic neurons labeled following injections of fluoro-gold in nucleus accumbens subterritories: Inverse relationship relative to known neurotoxin vulnerabilities. Brain Res. 1999; 844:67–77. [PubMed: 10536262]

Teng J, Takei Y, Harada A, Nakata T, Chen J, Hirokawa N. Synergistic effects of MAP2 and MAP1B knockout in neuronal migration, dendritic outgrowth, and microtubule organization. J. Cell Biol. 2001; 155:65–76. [PubMed: 11581286]

Tsou K, Brown S, Sanudo-Pena MC, Mackie K, Walker JM. Immunohistochemical distribution of cannabinoid CB1 receptors in the rat central nervous system. Neuroscience. 1998; 83:393–411. [PubMed: 9460749]

van Dongen YC, Mailly P, Thierry AM, Groenewegen HJ, Deniau JM. Three-dimensional organization of dendrites and local axon collaterals of shell and core medium-sized spiny projection neurons of the rat nucleus accumbens. Brain Struct. Funct. 2008

Vasquez C, Lewis DL. The CB1 cannabinoid receptor can sequester G-proteins, making them unavailable to couple to other receptors. J. Neurosci. 1999; 19:9271–9280. [PubMed: 10531431]

Villares J. Chronic use of marijuana decreases cannabinoid receptor binding and mRNA expression in the human brain. Neuroscience. 2007; 145:323–334. [PubMed: 17222515]

Voorn P, Gerfen CR, Groenewegen HJ. Compartmental organization of the ventral striatum of the rat: Immunohistochemical distribution of enkephalin, substance P, dopamine, and calcium-binding protein. J. Comp. Neurol. 1989; 289:189–201. [PubMed: 2478598]

Wang M, Ramos BP, Paspalas CD, Shu Y, Simen A, Duque A, Vijayraghavan S, Brennan A, Dudley A, Nou E, Mazer JA, McCormick DA, Arnsten AF. Alpha2A-adrenoceptors strengthen working memory networks by inhibiting cAMP-HCN channel signaling in prefrontal cortex. Cell. 2007; 129:397–410. [PubMed: 17448997]

Witkin JM, Tzavara ET, Nomikos GG. A role for cannabinoid CB1 receptors in mood and anxiety disorders. Behav. Pharmacol. 2005; 16:315–331. [PubMed: 16148437]

Zahm DS. Functional-anatomical implications of the nucleus accumbens core and shell subterritories. Ann. N. Y. Acad. Sci. 1999; 877:113–128. [PubMed: 10415646]
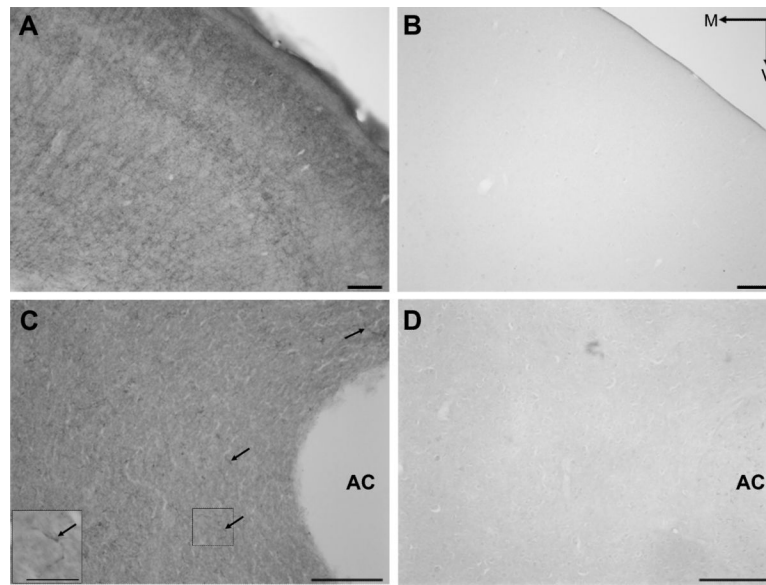
Figure 1.
Specificity of CB1R primary antibody. Brightfield photomicrograph showing immunoperoxidase labeling for CB1R in a cross section of the frontal cortex (FC, A) and the nucleus accumbens (Acb, arrows in C) of a wild-type mouse brain. Immunohistochemistry for CB1R in an equivalent cross section of a CB1R knock-out mouse reveals an absence of immunolabeling in the FC (B) and Acb (D). Inset in C shows higher magnification of CB1R-labelled fiber highlight in C. AC, anterior commissure; M, medial; V, ventral. Scale bar, 100μm.
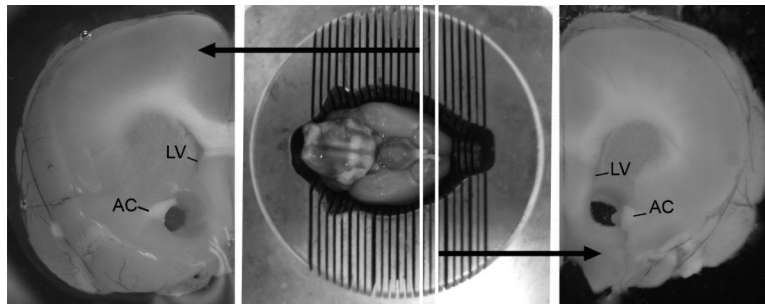
Figure 2.
Representative photomicrograph of the region of the nucleus accumbens (Acb) excised for protein analysis. A coronal section, ranging just rostral to the optic chiasm to 2mm anterior, was obtained in order to include the entire rostrocaudal extension of the Acb. Bilateral punches of the Acb were performed using a trephine medially to the anterior commissure (AC) and ventrally to the lateral ventricle (LV).
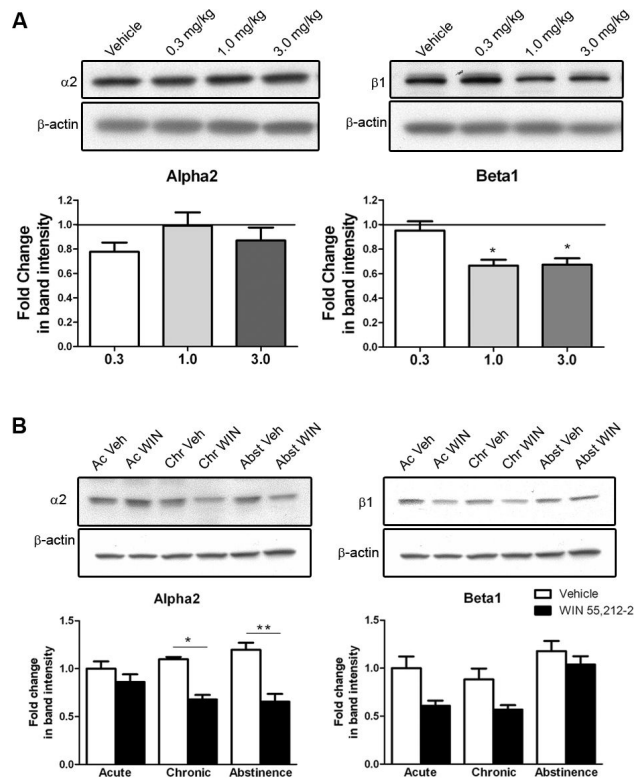
Figure 3.
Western blot for α2A and β1 adrenergic receptors (α2A- and β1-AR) from the nucleus
accumbens (Acb) following WIN 55,212-2 treatment. Bands shown are representative of
one sample from one animal of each group. **A.** Dose-response study showing that acute
administration of WIN 55,212-2 decreases the levels of β1-AR in the Acb at 1.0 and 3.0 mg/
kg (p<0.05). None of the doses used had an effect on the levels of α2A-AR. **B.** Western blot
for α2A-and β1-AR in protein extracts from the Acb of rats administered WIN 55,212-2 (3.0
mg/kg) or vehicle, acutely (one injection) or chronically (seven days) and euthanized 40 to
45 min or seven days (Chr+Abst group) after last injection. α2A-AR expression is not
altered by acute treatment with WIN 55,212-2. However, after chronic treatment (p<0.01),
there is a significant decrease in the expression of α2A-AR and this decrease persists in the
absence of the drug for seven days (Chr+Abst group) (p<0.001). Two-way ANOVA analysis
shows that β1-AR expression is significantly reduced after treatment with WIN 55,212-2
when compared to vehicle-treated animals. Data is represented as mean (+SEM) of fold
change in band intensity over the vehicle-treated animals, with acute vehicle-treated animals
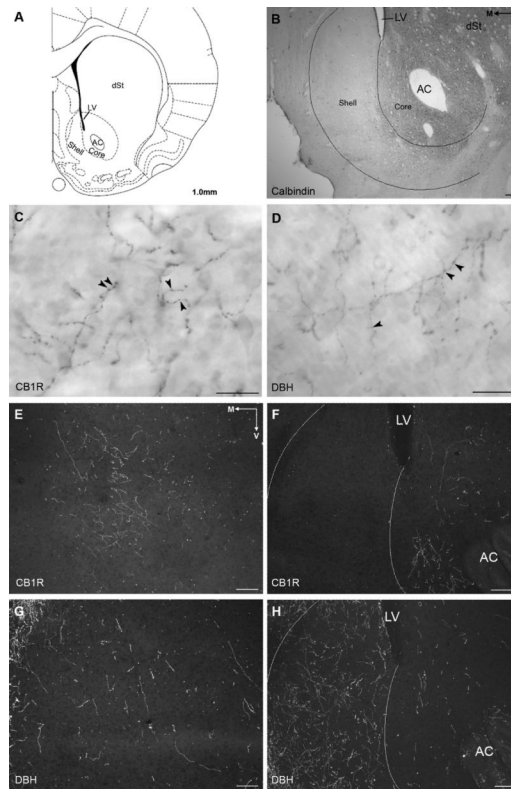set at 1.

Figure 4.
A. Diagram of a coronal section of rat forebrain adapted from the Rat Brain Atlas (Paxinos & Watson, 1997) showing subregions of the nucleus accumbens (Acb) in the ventral striatum. The core subregion of the nucleus accumbens surrounds the anterior commissure (AC) whereas the shell subregion is situated medial and ventral to the lateral ventricle (LV). **B.** Brightfield photomicrograph of calbindin immunoreactivity (calbindin-ir) in a coronal section of rat brain at an equivalent level to that shown in panel A. Calbindin-ir is more intense in the core and dorsal striatum (dSt) with almost no labeling in the shell. **C and D.** Brightfield photomicrographs from the shell of the Acb at approximately +1.7mm from bregma of CB1R and DBH-ir, respectively. High magnification of CB1R and DBH-ir shows tortuous and beaded (arrowheads) processes. **E and F.** Darkfield photomicrographs of CB1R-ir at two different levels of the Acb. CB1R-ir is seen in the shell at mid levels, approximately +1.7mm from bregma (E) and in the core at more caudal levels (+1.0mm from bregma) (F). At this level, CB1R-ir is almost completely absent from the dorsal shell (F). **G and H.** Darkfield photomicrographs showing DBH-ir at the same level of CB1R-ir in E and F, respectively. Some DBH-ir is seen at mid levels of the shell (G) and intense DBH-ir is seen in the shell at caudal levels (H). M, medial; V, ventral. Scale bar, 100μm except for C and D, scale bar, 25μm.
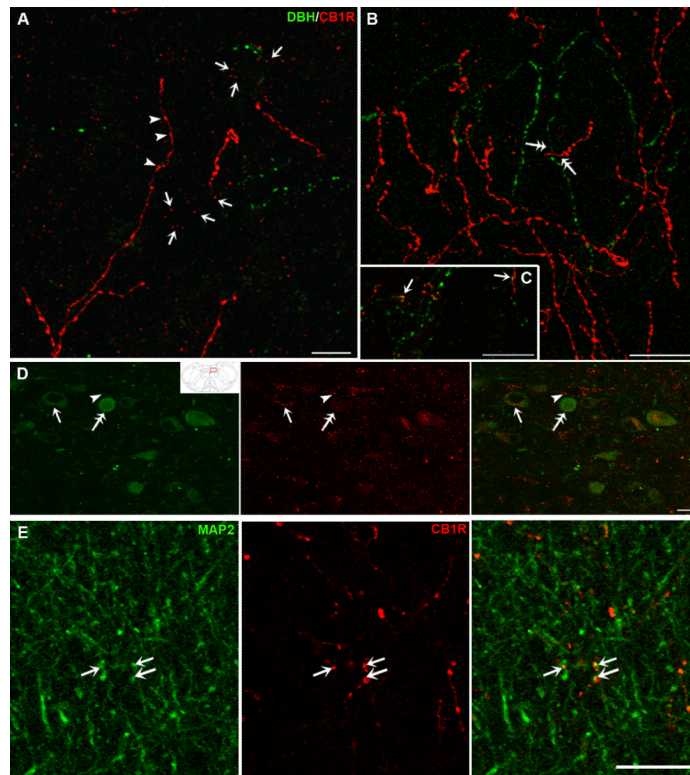
Figure 5.
Confocal fluorescence photomicrographs showing dual-labeling for CB1R and DBH in coronal sections of the nucleus accumbens (Acb, A–C) and the nucleus of the solitary tract (NTS, D) or CB1R and MAP2 in the Acb (E). CB1R was detected using a rhodamine isothiocyanate (red) conjugated secondary antisera and DBH and MAP2 were detected using a fluorescein isothiocyanate (green) conjugated secondary antisera. Inset represents a schematic diagram adapted from the Rat Brain Atlas (Paxinos & Watson, 1997) showing the level (−14.08mm from bregma) at which the photomicrograph was taken. **A–C.** CB1R and DBH-ir are frequently seen in the same field throughout the Acb. Both immunoreactivities show beaded processes resembling axonal structures (arrowheads in A) and punctate labeling consistent with post-synaptic profiles (arrows in A). Some co-localization of the two markers (arrows in C) can be seen. In addition, independently labeled fibers appear to converge on common structures (double arrows in B). **D.** CB1R immunoreactivity is associated with DBH-labeled neurons (arrow) as well as unlabeled neurons (arrowhead) in the NTS. Some of the DBH-labeled neurons lack CB1-ir (double arrows). **E.** Localization of CB1R in somatodendritic profiles labeled with MAP2 (arrows). Scale bar, 20μm.
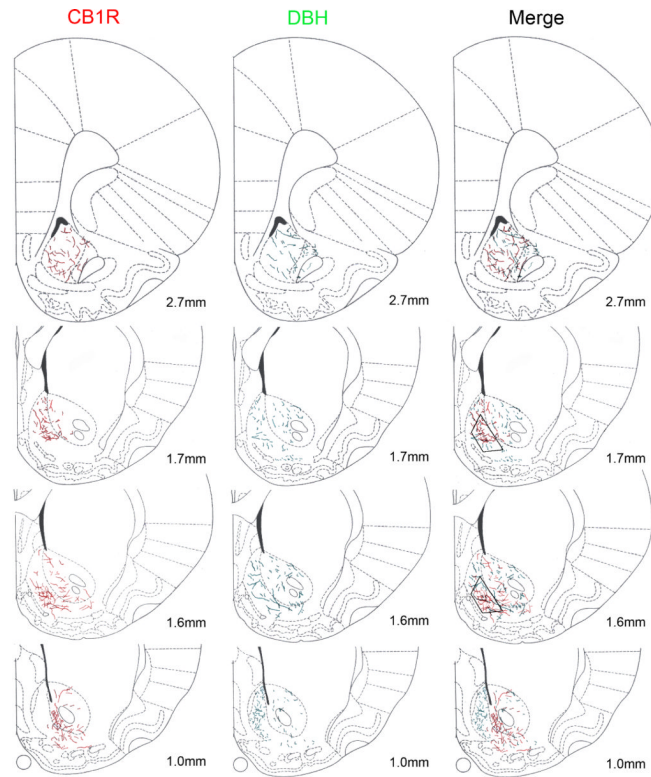
Figure 6.
Distribution of CB1R and DBH immunoreactivities along the extent of the nucleus accumbens (Acb) shown in schematics adapted from the Rat Brain Atlas (Paxinos & Watson, 1997). Distances shown represent location anterior to bregma. CB1R-ir is depicted in schematics on the left while DBH-ir is shown in schematics in the middle column. CB1R-ir is found diffusely in the core and in the shell subregions in the rostral third area of the Acb. At mid levels (1.7mm to 1.0mm), CB1R is found mainly in the shell and CB1R-ir shifts from the dorsal shell to the ventral shell, rostrocaudally. In the caudal third of the Acb (up to 1.0mm), CB1R-ir is almost exclusively found in the core. DBH-ir is found diffusely in the shell and core subregions with increased density as the nucleus progresses caudally. In the caudal third of the Acb (up to 1.0mm), DBH-ir is very intense in the shell and less so in the core. Trapezoids in the right column indicate the region sampled for ultrastructural analysis of CB1R and DBH distribution.
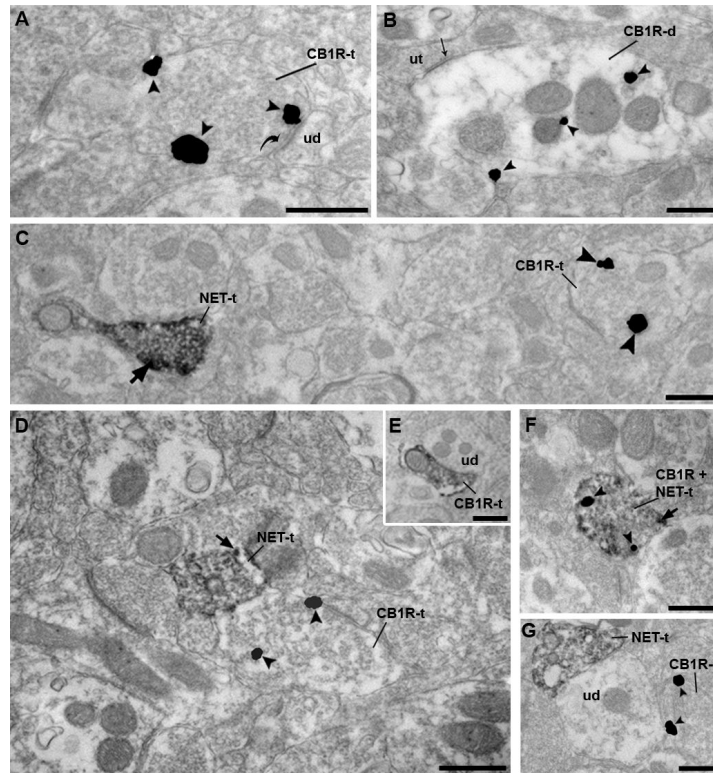
Figure 7.
Electron photomicrographs from the nucleus accumbens shell subregion showing immunogold-silver labeling (arrowheads) for CB1R and immunoperoxidase labeling for NET. Irrespective of whether the immunolabeling was in an axon terminal (A) or dendrite (B), immunogold-silver particles for CB1R could be detected within the cytoplasm as well as associated with the plasma membrane. **A**. Example of immunogold-silver labeling for CB1R in an axon terminal (CB1R-t) forming an asymmetric, excitatory-type synapse (curved arrow) with an unlabeled dendrite (ud). **B.** CB1R immunolabeling is present in a dendrite (CB1R-d) that receives a symmetric, inhibitory-type synapse (thin arrow) from an unlabeled terminal (ut). **C.** Dual localization of NET and CB1R using immunoperoxidase detection for NET and gold-silver labeling for CB1R. NET can be identified in an axon terminal by the presence of a diffuse peroxidase precipitate with intense immunoreactivity along the plasma membrane (thick black arrow). The immunoperoxidase-labeled NET axon terminal (NET-t) is found in the same field as a CB1R-t, that is labeled with gold-silver particles (arrowheads). **D.** A NET-t is apposed to an immunogold-silver labeled CB1R-t. **E.** Example of reverse labeling using immunoperoxidase for CB1R which is apposed to an unlabeled dendrite (ud). **F.** An example of an axon terminal that exhibits labeling for both CB1R and NET (CB1R+NET-t). **G.** An NET-t exhibiting immunoperoxidase labeling and a CB1R-t converging onto the same unlabeled dendrite (ud). Scale bar, 500nm.
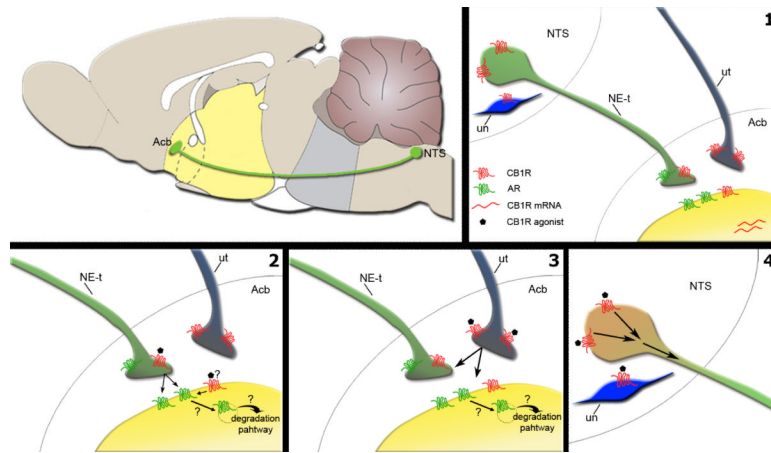
Figure 8.
Possible sites for modulation of noradrenergic transmission in the nucleus accumbens (Acb) by cannabinoids. **Left top panel.** Schematic of a saggital rat brain (Adapted by permission from Macmillan Publishers Ltd: Nature (Siegel, 2005), copyright (2005)) showing the noradrenergic input to the Acb arising from the nucleus of the solitary tract (NTS). **1**) The present study shows that in the Acb CB1R (in red) is found in noradrenergic terminals (NE-t), unlabeled terminals (ut) and in dendrites (in yellow). CB1R is also present in somatodendritic profiles of noradrenergic neurons and unlabeled neurons (un) in the NTS. Adrenergic receptors (in green) can be found pre- and pos-synaptically (MacDonald *et al.*, 1997; Ramos & Arnsten, 2007; Wang *et al.*, 2007). CB1R mRNA has been shown to be present in the Acb (Hohmann & Herkenham, 2000; Hurley *et al.*, 2003). We hypothesize that cannabinoids may modulate noradrenergic transmission in the shell of the Acb **2**) directly, through activation of CB1R present on noradrenergic terminals or dendrites. Whether dendritic CB1Rs are functional requires further studies. Nevertheless if functionally active, these receptors could impact adrenergic receptor expression; **3**) indirectly, through activation of CB1R in apposed terminals to noradrenergic terminals; **4**) indirectly, through activation of CB1R in the NTS neurons that send projections to the Acb.

Table 1

Characterization of the primary antibodies

Antigen	Immunogen	Manufacturer, host, mono/polyclonal	Catalog #	Dilution
Cannabinoid Receptor type 1 (CB1R)	Last 15 aa of the C-terminal of the rat CB1R	Synthesized in the laboratory of Dr. K. Mackie, rabbit polyclonal		1:500 1:1,000
Dopamine beta hydroxylase (DBH)	Purified bovine DBH	Chemicon, Millipore (Bedford, MA), mouse monoclonal	MAB308	1:1,000
Calbindin D-28	Purified calbindin D-28 from chicken gut	Abcam (Cambridge, MA), mouse monoclonal	ab9481	1:300
Norepinephrine transporter (NET)	Peptide, aa 5–17 of mouse and rat NET	Mab Technologies (Stone Mountain, GA), mouse monoclonal	NET05-1	1:1,000
α2A adrenergic receptor	Synthetic peptide, aa 218–235 of human, mouse, rat and pig	Sigma-Aldrich (St. Louis, MO), rabbit polyclonal	A-271	1:500
β1 adrenergic receptor	Synthetic peptide, aa 394–408 of mouse and rat	Sigma-Aldrich (St. Louis, MO), rabbit polyclonal	A-272	1:1,000
Microtubule associated protein (MAP2)	Rat brain MAP	Abcam (Cambridge, MA), mouse monoclonal	ab11267	1:1,000